Cleaner Logistics and Supply Chain 10 (2024) 100144

Contents lists available at ScienceDirect

Cleaner Logistics and Supply Chain

journal homepage: www.journals.elsevier.com/cleaner-logistics-and-supply-chain

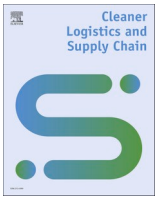

A robust Logistics-Electric framework for optimal power management of electrified ports under uncertain vessel arrival time

Ilias Sarantakos [a], Saman Nikkhah [a,*], Meltem Peker [b], Annabel Bowkett [a], Timur Sayfutdinov [c], Arman Alahyari [a], Charalampos Patsios [a], John Mangan [a], Adib Allahham [d], Eleni Bougioukou [e], Alan Murphy [a], Kayvan Pazouki [a]

[a] School of Engineering, Newcastle University, Newcastle upon Tyne, United Kingdom
[b] Department of Industrial Engineering, Bilkent University, Ankara, Turkey
[c] School of Advanced Technology, Xi'an Jiaotong-Liverpool University, Suzhou, China
[d] Faculty of Engineering and Environment, Northumbria University, Newcastle upon Tyne, United Kingdom
[e] Port of Tyne, Maritime House, Tyne Dock, South Shields Newcastle upon Tyne, United Kingdom

ARTICLE INFO

Keywords:
Port electrification
Robust optimisation
Logistic-electric operation
Uncertainty

ABSTRACT

Maritime transport is responsible for producing a considerable amount of environmental pollution due to the reliance of ports and ships on the carbon-based energy sources. With the increasing trend towards port electrification to reduce carbon emissions, the operation of ports will be increasingly relying on the electricity network. This interconnection creates multiple challenges due to the complexity of power flow in the port network, uncertainty of vessel arrival time and fluctuation of power generation of renewable energy sources. These uncertainties can lead to an overload in electricity networks and delays in cargo-handling activities, resulting in increased vessel handling times and environmental emissions. This paper presents a joint logistics-electric framework for optimal operation and power management of electrified ports, considering multiple uncertainties in the arrival time of vessels, network demand, and renewable power generation. An optimal power flow method is developed for a real-life port, with consideration for multiple port logistic assets such as cargo handling equipment, reefers, and renewable energy sources. The proposed model ensures feasible port operation for all uncertainty realisations defined by robust optimisation, while minimising operational costs. Simulation results demonstrate that the probability of a network constraint violation can be as high as 70% for an electrified major UK port if the uncertainty in the port operation is neglected, presenting an unacceptable risk of disruption to port activities. Furthermore, such uncertainty can cause 150% increase in emissions if the ships use their auxiliary engine instead of using shore power. The numerical study shows that such challenges can be handled by a 0.3% increase in the robustness in face of uncertainty, while the cost increase in the worst case does not exceed 4.7%. This shows the effectiveness of the proposed method enhancing robustness against uncertainty at the minimum cost.

1. Introduction

Maritime transportation accounts for approximately 80 %-90 % of global trade, and is responsible for producing 2.5 % of global greenhouse gas emissions (Chua et al., 2023). These figures can increase up to 44 % by 2050 if no appropriate actions are taken according to the International Maritime Organization (IMO) (International Maritime Organisation, "Fourth IMO GHG Study,", 2020). Ports play a key role in achieving the 2050 maritime transportation net zero emissions which is a strategic ambition of many governments and other stakeholders (e.g. the UK government's Clean Maritime Plan (Department for Transport, 2019). Achieving such an ambitious plan, however, requires significant investment in ports along with investment from ship owners and bunker fuel suppliers. Thus, one of the critical steps towards realising net zero targets is port electrification.

Abbreviations: IMO, International Maritime Organization; FLTs, Forklift Trucks; CHE, Cargo Handling Equipment; EVs, Electric Vehicles; IEVs, Industrial Electric Vehicles; RLE, Robust Logistic-Electric; PoT, Port of Tyne; CCG, Column and Constraint Generation; MP, Master Problem; SP, Subproblem; MGO, Marine Gas Oil; PoCV, Probability of Constraint Violation.

* Corresponding author.
E-mail address: saman.nikkhah@newcastle.ac.uk (S. Nikkhah).

https://doi.org/10.1016/j.clscn.2024.100144
Received 6 November 2023; Received in revised form 9 January 2024; Accepted 15 January 2024
Available online 18 January 2024

Nomenclature

Sets

A_j	Set of nodes connected to node j except its parent node.
D^t	Uncertainty set of nodal net injection at time t.
Ω_b, Ω_n, Ω_t	Set of network branches / nodes / time periods.
$\Omega_{b,SS}$	Set of network branches connected to the substation busbar.
$\Omega_{n,sp/c}$	Set of network nodes that supply shore power demand or cranes.
Ω_V	Set of vessels served by cranes (container ship, biomass carrier, plywood carrier).
Ω_e	Set of industrial EVs
Ω_c	Set of cranes.
Ω_q	Set of reefers.

Indices

i, j	Indices of nodes/buses (i, $j \in \Omega_n$).
ij	Index of branch ij ($ij \in \Omega_b$).
r	Index of realization for uncertain vessel arrival times.
t	Index of time.
v	Index of vessels served by cranes.
c/e	Index of cranes/industrial EVs.
q	Index of reefers.

Variables

$\gamma^C_{c,v,t}$	Binary variable indicating the operation of the crane c for vessel v at time period t.
d^t_i	Uncertain net injection of node i at time t.
$I_{ij,t}$	Current magnitude of branch ij, at time t.
$L_{ij,t}$	Squared current magnitude of branch ij at time t.
$P_{ij,t}$, $Q_{ij,t}$	Active/Reactive power flow from node i to j, at time t.
$P^{cr}_{c,v,t}$	Average power consumption of crane c for unloading vessel v during time t.
$P^{\mathrm{ES}_{ch}}_{j,t}/P^{\mathrm{ES}_{dch}}_{j,t}$	Charging/Discharging power of energy storage.
$P^{\mathrm{EV}_{ch}}_{e,t}$	Charging power of all industrial EV e of a specific category (i.e., container tractors, reach stackers, empty handlers, trucks, forklift trucks).
$P^{\mathrm{EV}_{op}}_{\mathrm{e},t}$	Power consumption of operating industrial EV.
$P^{\mathrm{CHE}}_{j,t}$	Total power consumption from all cargo handling equipment (i.e., cranes, hoppers, and industrial EVs) at bus j at time t.
$P^{\mathrm{Reef}}_{q,t}$	Reefer power consumption at time t.
$P^{\mathrm{Reef}}_{j,t}$	Cumulative power consumption of all reefers at bus j.
$\mathrm{SOC}^{\mathrm{ES}}_{j,t}$	State of charge of energy storage installed in bus j at time t.
$\mathrm{SOC}^{\mathrm{EV}}_{e,t}$	State of charge of all industrial EVs of a specific category.
$V_{i,t}$, $u_{i,t}$	Voltage magnitude / Squared voltage at node i, time t.
$\mathrm{P}^{VL}_{v,t}$	Vessel load for each vessel v at time step t.
$w_{v,r}$	Binary variable which indicates the selected realization r for the uncertain arrival time of vessel v.
$\zeta^{ES}_{j,t}$	Binary variable indicating the state of charge of energy storage.
γ, $I_{i,t}$	Auxiliary binary variables used to define the uncertainty set.
$\theta_{q,t}$	Internal temperature of the reefer r at time t.

Parameters

cd_v	Call duration of vessel v.
$\overline{d}^t_i$	Nominal value of the net injection of node i at time t.
$\widehat{d}^t_i$	Deviation from the nominal net injection for node i at time t.
$I_{ij,\ \max}$	Ampacity of branch ij.
LF^{EV}_e	Load factor of industrial EV.
$N^{\mathrm{IEV}}_{\mathrm{total}}$	Total number of industrial EVs of a specific category.
$N^{\mathrm{EV}}_{\mathrm{c}}$	Number of industrial EVs (of a specific category) per operating crane.
N_{r}	Number of possible realisations for uncertain vessel arrival times.
N^{w}_v	Number of staff required per operating crane for vessel v.
$P^{\mathrm{D}}_{i,t}$, $Q^{\mathrm{D}}_{i,t}$	Active / Reactive power demand at node i, time t.
$P^{\mathrm{G}}_{i,t}$, $Q^{\mathrm{G}}_{i,t}$	Active / Reactive power generation at node i, at time t.
$P^{\mathrm{ES}}_{\max}$	Power rating of energy storage.
$P^{\mathrm{EV}^{\max}_{op}}_e$	Maximum power of each unit of a specific industrial EV category.
$P^{\mathrm{Reef}_{\max}}_q$	Maximum power consumption of reefer.
$P^{\max}_c$	Maximum crane power consumption.
Π^{oe}_t	Price of electricity and environmental emission at time t.
R_{ij}, X_{ij}	Resistance / Reactance of branch ij.
$\mathrm{SOC}^{\mathrm{ES}_{\max}}_j$	Maximum state of charge of energy storage.
$\mathrm{SOC}^{\mathrm{EV}_{\max}}_e$	Maximum state of charge of each unit of a specific industrial EV category.
T	Number of time periods.
$t_{\mathrm{arr},v}$, $t_{\mathrm{dep},v}$	Arrival and departure time of vessel v.
U_{at}	Uncertainty of vessel arrival times.
$V_{\max}$, $V_{\min}$	Maximum and minimum voltage limit.
$\mathrm{VL}_{v,\mathrm{init}}$	Initial load of vessel v.
wc	Workforce cost
Δt	Duration of a single time period.
η^{EV}_e	Battery efficiency of industrial EVs.
η^{ES}_j	Battery energy efficiency of energy storage installed at bus j.
θ^{amb}_t	Reefer ambient temperature at time t.

Additional load from electrification will clearly have a significant impact on port electricity networks, in terms of capacity and voltage limits. This impact is further exacerbated by uncertainty – not only around expected levels of network demand and renewable power generation – but also, and most importantly, by port operation such as uncertainty in the vessel arrival time. For example, if the departure of a ship and the arrival of another are expected to be temporally close to each other, a potential overlap even for one hour could lead to a significant overload on the port's electricity network due to the need for using shore power. Therefore, in an electrified port, port operation can have major risks to both the port's operational performance and the integrity of its electrical infrastructure. Furthermore, the delay in supplying the ships through cold ironing can have a major environmental impact due to the need for running the ships' auxiliary engines while waiting to be served. More dramatically, as shore power gets greener, the emissions from not connecting to shore power because of uncertainty in arrival time of vessels will rise.

These challenges (i.e. electrification of port networks and uncertainties in port logistics operations) initiates the necessity of a framework for port operation. Such a framework could be applicable for electrified ports, while taking the uncertainty of different parameters (e.g. vessel arrival time, renewable power generation, etc.) into account.

1.1. Literature review

Existing research focuses on either the logistics and operations activities of ports (e.g. (Giallombardo et al., 2010) or the power management of ports (e.g. (Sun et al., 2022). Operational activities have been

dependent on heavy fuel oil (for ships) and diesel (for port equipment), rather than electrical supplies. However, with the increasing trends towards port electrification to reduce carbon emissions, the interaction of ships and ports will not only be governed by operational constraints but also by the power flow constraints imposed by the port's electricity network (Fang et al., 2020). Two major examples of port electrification are: 1) shore power (ships are supplied from the port electricity network to satisfy their 'hotel' demand (e.g. lighting, air conditioning) and 'mission' load (systems and machinery for cargo storage and transfer) while at berth and with their engines switched off), and 2) electrification of port cargo handling equipment (Frontier, 2019). This leads to the concept of the electrified port, where all berthed vessels and cargo handling equipment (where technically feasible) are supplied by the port's electricity network. The literature review is conducted based on existing studies in the field in available databases. The available research works are categorised into a) the logistics-based operation, and b) electric power management of ports. This categorisation enabled a systematic analysis of available literature to understand the gaps and develop a comprehensive operation model.

1.1.1. Logistics-based operation

In this study, the term 'logistics' is used to refer to the operations required to unload cargo from a berthed vessel and transfer it to the required location within the port, e.g., to the container yard, warehousing, or transit sheds. This requires managing the operation of various types of port assets such as cranes, hoppers, trucks, container tractors, reach stackers, empty handlers, forklift trucks (FLTs), etc. These assets are referred to as cargo handling equipment (CHE) in the rest of this paper. Optimal CHE scheduling is required to minimise overall costs while increasing cargo throughput, and thereby ensure a successful and effective operation of the port. Strategies to achieve this include optimising resource utilisation (berths, CHE, workforce) and reducing vessel handling times (Bierwirth and Meisel, 2015), all of which can result in increased productivity and operational efficiency.

Research in this area (Giallombardo et al., 2010; Agra and Oliveira, 2018) originally focused on crane scheduling and berth allocation mainly for container terminals. Nowadays, increasing fuel prices and the necessity of reducing environmental emissions have made energy consumption one of the top concerns of ports (Dulebenets, 2022), resulting in an expansion of CHE scheduling problems to include energy-aware optimisation of operations (Iris and Lam, 2019). Objectives of such optimisation problems include minimising energy consumption and emissions, which could be achieved, e.g., through CHE routing to reduce distance travelled (Sha, 2017). Hu *et al.* (Hu et al., 2014) propose a multi-objective mixed-integer programming model to solve the integrated berth allocation and quay crane assignment problem with consideration for vessel fuel consumption and emissions, while improving berth and crane utilisation and maintaining service quality. The impact of the number of quay cranes allocated to a vessel on port operational costs and vessel fuel consumption and emissions is also analysed. References (He et al., 2015; Liu and Ge, 2018; Yue et al., 2024; Kenan et al., 2022) have incorporated energy consumption and emissions into quay crane allocation and scheduling problems, while extending to decision making for other port CHE, such as yard cranes and trucks. The majority of the literature in this context (e.g. references (Liu and Ge, 2018), and (Yue et al., 2024) considers berthed vessels use their auxiliary engines to power onboard CHE or diesel-powered CHE available at quayside which can bring about considerable emissions.

1.1.2. Electric power management

Energy efficient policies and operations achieve worthwhile but limited emissions reductions, especially when applied to ships and CHE fuelled by carbon-based energy sources. To achieve emissions reductions by nowadays standards, alternative methodologies should be applied to achieve a balance between cost and environmental benefits (Peng et al., 2021). Electrification is one such solution and decarbonisation of national electricity supplies through the introduction of renewable energy generation is further increasing its emissions reduction efficacy. Electrifying port energy demand can increase the wind power penetration in the energy network due to the fact ports are extended along the coastline, which is a potential location for offshore wind turbines.

With shore power and CHE electrification being implemented at ports globally and in the UK, research on the problems of port power and energy management is growing, not only to identify methods to manage the significant additional demand these technologies will place on port power networks, but also to maximise benefits from flexibility and enhanced controllability delivery by digitalisation. References (Sun et al., 2022; Yu et al., 2022; Kanellos et al., 2019; Wang et al., 2022) considered shore power and electrification of some CHE, although emission reduction has not been considered in all of them. Sun *et al.* (Sun et al., 2022) investigated optimal voltage control and berth allocation in a port microgrid, accounting for cranes but without scheduling their operation and without considering other CHE. Reference (Yu et al., 2022) utilised a similar approach while accounting for emission reduction. In (Kanellos et al., 2019), a multi-agent optimisation is used for the port power management considering the loads of shore power, refrigerated containers (reefers), and electric vehicles (EVs) but without modelling the operation of CHE. Wang *et al.* (Wang et al., 2022) studied the day-ahead optimal scheduling of ports with the aim of reducing energy costs and carbon emissions, by considering gas and hydrogen and taking CHE into account. The explicit assets operation has been neglected by the authors, while the connectivity with the vessel operation is also missing in the optimisation model.

Finally, the effect of uncertainty on the optimal operation of electrified ports has not been considered in the majority of the literature, which may result into the electrical demand of the ports exceeding capacity limits if not carefully scheduled. Although Zhang *et al.* (Zhang et al., 2022) investigated the effect of uncertainty on the port operation, the lack of electricity network, however, the authors have not demonstrated the effect of uncertainty on network overloads and voltage limits. Neglecting vessel arrival time is another missing aspect in the literature (Zhang et al., 2022). The importance of uncertainty in vessel arrival time is shown in (Norlund and Gribkovskaia, 2017). To this end, frequent schedule changes are the last thing port planners want to see (Liu et al., 2017). This could be because of a potential network overload, especially in electrified ports, where the prevention of which could result in reduced CHE and workforce utilisation and increased carbon emissions due to extended vessel waiting times. The latter is a substantial concern as the auxiliary engine's emissions could be as high as 722 g/kW-hr CO_2 production (Nguyen et al., 2022) due to the delay in supplying the ships with shore power.

2. Research gap

The majority of literature on optimising the scheduling of port operations (He et al., 2015; Liu and Ge, 2018; Yue et al., 2024) considered berthed vessels using their auxiliary engines which can produce a sizable amount of environmental pollution. Although recent studies have started to incorporate emissions and energy consumption into the scheduling problems (Sha, 2017; Hu et al., 2014; He et al., 2015; Liu and Ge, 2018; Yue et al., 2024; Kenan et al., 2022), the majority of these research works focus on large container terminals and carbon-based fuels rather than ships supplied by shore power and electrified CHE. Furthermore, the literature on multipurpose ports is lacking, basically because such ports have diverse cargo mixes and different types of vessels, CHE, and port facilities, resulting in more variable shore side activities and less predictable energy demand. On the power management side (Yu et al., 2022; Kanellos et al., 2019; Wang et al., 2022), optimal power and energy management of ports is a relatively new and fast developing research area. Most of the literature so far have considered energy costs (Wang et al., 2022), optimal energy management including renewables

and storage (Kanellos et al., 2019), and – more recently – reducing emissions (Yu et al., 2022), but few studies considered the physical and operational constraints of electricity network in conjunction with logistics operation of ports and CHE scheduling. Finally, concerning the impact of uncertainty (Zhang et al., 2022), there is a notable absence of analysis on how the uncertainty in vessel arrival time influences power operations. In summary, the following gaps are observed based on the literature:

- With the increasing interests in electrification of ports (Sarantakos, 2023), the coordination of port assets and the requirement of electricity network could be the key for avoiding reinforcement. There is a scarcity of literature that deals with the near future interdependency between the operations of ports (vessel unloading and cargo handling activities) and their electricity networks. This leaves electrified ports vulnerable by having their operations, and thus commercial performance and competitiveness, dependent on the ability of their electricity network to meet the required power demand at any given time. Therefore, a comprehensive logistic-electric port operation model is required to investigate the interdependency of port and its electricity network.
- Uncertainty associated with the operation of electrified ports is another challenge which requires further investigation. For example, if uncertainty of vessel arrival times is not considered, cargo handling activities would have to be delayed, resulting in increased vessel handling times and emissions, and significantly reduced service levels.
- Studies on optimising port operations and CHE scheduling, including those that also aim to reduce emissions and energy consumption are limited mainly to large container terminals. Few (if any) consider smaller multipurpose ports which represent the majority of UK ports, and also need to be considered if UK maritime decarbonisation targets are to be achieved.

For port electrification to successfully contribute its full potential to maritime decarbonisation through coordination of assets, it is essential that the additional demand placed on port electricity networks does not disrupt port operations or have a detrimental effect on port performance. Thus, studies that investigate the multipurpose port operation are required to address the above research gaps by: 1) modelling and scheduling of electrified port CHE and their impact on port electricity networks, and 2) considering the impact of uncertainty (especially vessel arrival time uncertainty) on the operation of electrified ports. Such a framework could be an alternative for the port reinforcement which can cause considerable planning costs.

2.1. Contributions

This study attempts to fill the aforementioned gaps by proposing a robust logistic-electric (RLE) scheduling strategy to optimise the operation of multipurpose all electric ports with consideration for uncertainty in the vessel arrival time. The impact of neglecting the uncertainties in optimising the operation of all electric ports is demonstrated, while a RLE based framework is developed to appropriately manage uncertain vessel arrival times as well as uncertain levels of network demand and renewable power generation. The proposed RLE framework optimises the logistics operation ports including cranes, CHE, and reefers, with the aim of minimising the total operation costs (comprising energy, carbon emissions, and workforce costs) while ensuring that network limits are not violated in the presence of uncertainty. Multiple network loads including shore power, electrified CHE (multiple types, including mains connected and battery-powered, which correspond to the specific operations for unloading and handling a range of cargoes from different types of vessels), and the refrigeration demand of reefers, as well as energy storage and renewable power generation are considered in the operation of the electric port. The proposed method is tested on Port of Tyne (PoT) (Sarantakos, 2023), as a real-life port to validate the efficiency of the proposed optimisation. Generally, the main contributions of the paper are therefore as follows:

- Introducing robust logistic-electric (RLE) optimisation framework for electrified ports, considering shore power and electrified CHE. The proposed framework links the power flow of electric power network of the electrified ports to the logistic operation to explore flexibility that can be enabled through optimal control of different port assets.
- Addressing the uncertainty of vessel arrival time as a critical challenge affecting the realisation of the network constraint in optimal operation of electrified ports. The proposed framework demonstrates the substantial consequences of neglecting potential uncertainties in the optimal operation of all electric ports and introduces a set of constraints into the optimisation problem to prevent the violation of network constraints under the influence of multiple uncertainties, specifically vessel arrival time. The proposed method shows how flexible assets within a port can improve the system robustness in face of uncertainty in arrival time of vessels.
- Developing a convex multi-level optimisation problem for optimal operation of all electric ports to ensure viability (in terms of achieving optimality) of the results for a real-life port system.

These contributions aim to address the research gap identified in Section 1.2. Table 1 provides a summary of the relationship between each research gap and the contributions of this study.

The rest of this paper is organized as follows. Section 2 presents the mathematical formulation used for modelling the proposed logistic-electric port operation. Section 3 presents the associated problem formulation with uncertainty. Section 4 defines the solution methodology. Section 5 provides an overview of the PoT network and the data associated with its operation. Section 6 illustrates the corresponding simulation results. Finally, Section 7 draws the conclusions of this paper.

3. Mathematical description of port operation

The operational processes that follow the arrival of each vessel type are described in this section. When a vessel arrives at the container terminal, containers are unloaded by the port's cranes onto container tractors, which transport them to the container yard; there, reach stackers and empty handlers stack and position containers as required. The biomass cargo handling operation is shown in Fig. 1, where cranes lift the biomass from the vessel's holds into hoppers on the quay and is then transferred via trucks to a warehouse. Subsequent rail transport to the power station is not included in this modelling. Regarding plywood,

Table 1
Alignment of research gap and contributions of this study.

Research gap	Contribution of the paper towards the gap
o There is a lack of literature addressing the imminent interdependence between port operations and their associated electricity networks.	o Presenting a RLE optimization framework for electrified ports, considering shore power and electrified CHE, linking the electric and logistic operation of ports.
o Studies focused on optimizing port operations and CHE scheduling are predominantly confined to large container terminals, with minimal attention given to smaller multipurpose ports.	o Developing a convex multi-level optimization problem for the optimal operation of all-electric ports to ensure practical applicability for real-life multipurpose ports.
o The uncertainty of vessel arrival times is not considered in the literature, which can lead to several challenges such as delayed cargo handling activities, and elevated emissions.	o Addressing the uncertainty of vessel arrival time, a critical challenge impacting network constraints, by introducing constraints to prevent violations under multiple uncertainties.

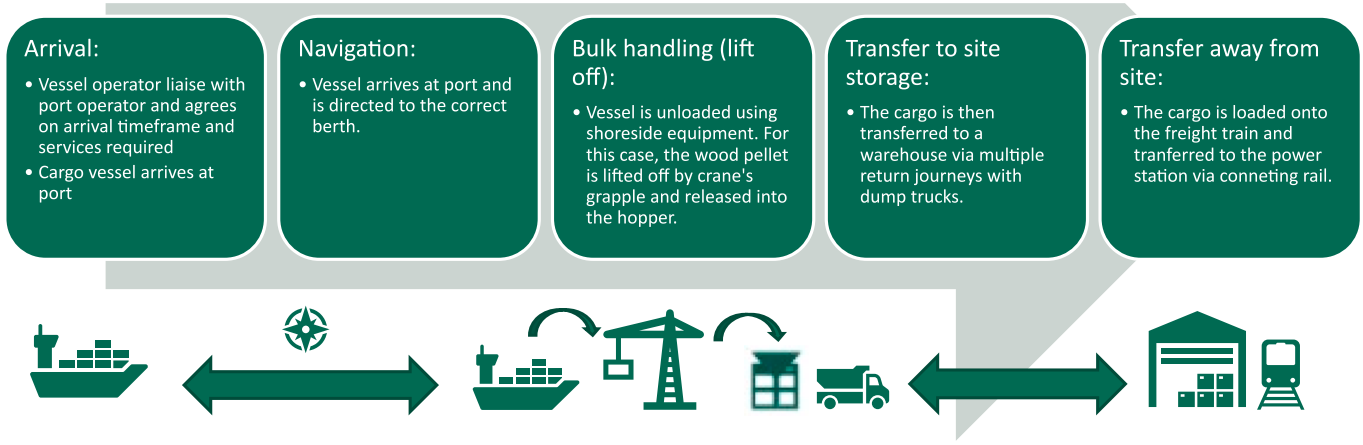

Fig. 1. Port operations following the arrival of a bulk carrier, transporting biomass in the form of wood pellets (Catapult, 2021).

cranes unload the cargo onto the quay, where it is transported to storage using the port's FLTs. Finally, the car terminal operations involve only shore power equipment in this modelling, as cars are driven on/off the vessel and parked in the terminal without the use of any CHE.

This section introduces the mathematical representation of the proposed logistics-electric port operation model based on the operational process described above. The objective function, port electric network constraints, and logistic model of different port assets are described in this section. The proposed RLE optimization framework is based on the following assumptions:

The call duration of vessels at berth remains constant.
The maximum uncertainty around the arrival time of vessels is limited to two hours.
The port operator possesses the authority for optimal electric power management of the port.
Efficient CHE is accessible in the port to unload vessels during their time at berth.

3.1. Objective function

The objective function of the proposed optimisation model is composed of the workforce cost, and operational cost of electricity and carbon emissions, as represented below:

$$\min \underset{DV}{OF} = \sum_{t\in\Omega_t}\Delta t\left\{\left[\sum_{c\in\Omega_c}\sum_{v\in\Omega_v}\left(\mathrm{wc}\times N_v^{\mathrm{w}}\times\gamma_{c,v,t}^{C}\right)\right]+\left[\sum_{ij\in\Omega_{\mathrm{b,SS}}}\left(\Pi_t^{oe}\times P_{ij,t}\right)\right]\right\} \tag{1}$$

where the first term represents the workforce cost based on the number of staff required per operating crane (i.e.N_v^{w}). The binary variable $\gamma_{c,v,t}^{C}$ represents the operation of cranes while *wc* is the workforce cost parameter. The second term in (1) represents the operational cost of electricity and carbon emissions., where Π_t^{oe} is the price of electricity and environmental emission at time *t* and $P_{ij,t}$ is active power flow from node *i* to *j*, at time *t*.

3.2. Port electricity network constraints

The port network is a low voltage network, with logistic assets as the consumers and possible small-scale generation units. The port network is modelled using DistFlow branch equations which is convexified using the method described in (Farivar and Low, 2013). The port power flow equations are modelled based on Fig. 2. Based on this figure, the active (and reactive) power flow at the sending node of branch *ij* equals the: a) sum of power flows from node *j* to nodes *k1, k2,*…, kn, b) branch losses, and c) demand at node *j* minus generation capacity at node *j* (Baran and Wu, Apr. 1989). Accordingly, the port power flow equations are modelled as below:

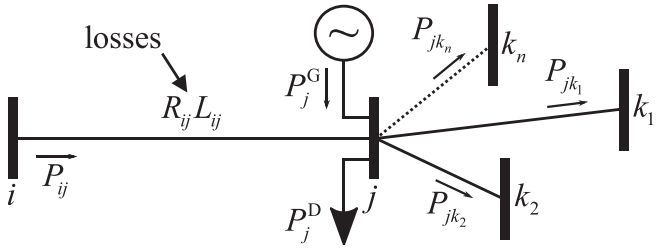

Fig. 2. Graphical representation of the *DistFlow branch equations*.

$$P_{ij,t} = \sum_{k\in A_j} P_{jk,t} + R_{ij}L_{ij,t} + P_{j,t}^{\mathrm{D}} - P_{j,t}^{\mathrm{G}}, \forall ij \in \Omega_{\mathrm{b}} \tag{2}$$

$$Q_{ij,t} = \sum_{k\in A_j} Q_{jk,t} + X_{ij}L_{ij,t} + Q_{j,t}^{\mathrm{D}} - Q_{j,t}^{\mathrm{G}}, \forall ij \in \Omega_{\mathrm{b}} \tag{3}$$

$$u_{j,t} = u_{i,t} - 2\left(R_{ij}P_{ij,t} + X_{ij}Q_{ij,t}\right) + \left(R_{ij}^2 + X_{ij}^2\right)L_{ij,t}, \forall ij \in \Omega_{\mathrm{b}} \tag{4}$$

$$u_{i,t} = V_{i,t}^2, \forall i \in \Omega_{\mathrm{n}} \tag{5}$$

$$L_{ij,t} = \left(P_{ij,t}^2 + Q_{ij,t}^2\right)\Big/ u_{i,t} = I_{ij,t}^2, \forall ij \in \Omega_{\mathrm{b}} \tag{6}$$

$$V_{\min}^2 \leqslant u_{i,t} \leqslant V_{\max}^2, \forall i \in \Omega_{\mathrm{n}} \tag{7}$$

$$L_{ij,t} \leqslant I_{ij,\max}^2, \forall ij \in \Omega_{\mathrm{b}} \tag{8}$$

Where (2) and (3) represent the active and reactive power flow at sending node of branch *ij*. Parameters R_{ij} and X_{ij} are resistance and reactance of branch between buses *i* and *j*. Variable $u_{i,t}$ and $L_{ij,t}$ in (4) are defined to facilitate the convex formulation of the power flow model. The former is defined based on voltage magnitude in Equation (5) while the latter is defined in constraint (6) based on active and reactive power flow at sending node of branch *ij*. Finally, constraints (7) and (8) represent the limits on $u_{i,t}$ and $L_{ij,t}$.

These equations are referred to as the relaxed branch flow equations. Eq. (6) turns the optimisation problem into a nonconvex model due to the quadratic terms in this equation. Therefore, it has been relaxed to (Farivar and Low, 2013):

$$\left\| 2P_{ij,t} \quad 2Q_{ij,t} \quad L_{ij,t} - u_{i,t} \right\|_2 \leqslant L_{ij,t} + u_{i,t} \tag{9}$$

Incorporating energy storage, CHE comprising of both mains-connected cranes and hoppers as well as battery-powered industrial EVs (e.g. container tractors, reach stackers, empty handlers, trucks, forklift trucks), and reefers into the port network, equations and can be modified as below:

$$P_{ij,t} - \sum_{k:j\to k} P_{jk,t} - R_{ij}L_{ij,t} = P^{\mathrm{D}}_{j,t} - P^{\mathrm{G}}_{j,t} + P^{\mathrm{ES}_{ch}}_{\mathrm{j,t}} - P^{\mathrm{ES}_{dch}}_{j,t} + P^{\mathrm{CHE}}_{j,t} + P^{\mathrm{Reef}}_{j,t}, \forall ij \in \Omega_{\mathrm{b}} \tag{10}$$

$$Q_{ij,t} - \sum_{k:j\to k} Q_{jk,t} - X_{ij}L_{ij,t} = Q^{D}_{j,t} - Q^{G}_{j,t} - Q^{\mathrm{Reef}}_{j,t}, \forall ij \in \Omega_{\mathrm{b}} \tag{11}$$

These constraints represent the power flow equations based on the active/reactive power of different logistic-electric assets in the port. Note that the power consumption of CHE is comprised of the power consumption of cranes, and charge discharge power of industrial EVs, as defined below:

$$P^{\mathrm{CHE}}_{j,t} = \sum_{c\in\Omega_c}\sum_{v\in\Omega_v}(P^{cr}_{c,v,t}) + \sum_{e\in\Omega_e}\sum_{c\in\Omega_c}\left(P^{EV_{ch}}_{e,t}\right) \tag{12}$$

where Ω_e is the set of industrial EVs (of a specific category) per operating crane, e.g., three for container tractors. In the following, the logistic-electric operational models of different assets are described.

3.2.1. Cranes

Cranes are one of the main elements of ports and play a vital role in cargo movements inside the port. The operation of cranes depends on the arrival of vessels in the port, i.e., the cranes start operating if the vessels are available to unload. Therefore, in this study the crane's operation is modelled based on vessel load, as below:

$$\mathrm{P}^{VL}_{v,t+1} = \mathrm{P}^{VL}_{v,t} - \sum_{c\in\Omega_c} P^{cr}_{c,v,t} \tag{13}$$

$$\mathrm{P}^{VL}_{v,t1} = \mathrm{P}^{VL}_{v,t_{init}} \tag{14}$$

$$\mathrm{P}^{VL}_{v,t_{end}} = 0 \tag{15}$$

$$0 \leqslant P^{cr}_{c,v,t} \leqslant \gamma^{C}_{c,v,t} \times P^{\max}_{c} \tag{16}$$

$$\gamma^{C}_{c,v,t} = 0, \forall t \notin [t_{\mathrm{arr},v}, t_{\mathrm{dep},v}] \tag{17}$$

Eq. (13) relates the vessel load (i.e. $\mathrm{P}^{VL}_{v,t}$) to the operation of the cranes (i.e. $P^{cr}_{c,v,t}$). It should be noted that these equations apply to those vessels for which cranes are used to handle their load (i.e. all vessels except car carriers). The initial load of each vessel is given in. Without loss of generality, it has been assumed that each vessel has an initial load that needs to be unloaded, as indicated by constraint. Constraint represents the maximum power consumption of cranes based on their operation status (i.e. in operation if $\gamma^{C}_{c,v,t} = 1$, and not operating if $\gamma^{C}_{c,v,t} = 0$). Finally, constraint (17) indicates that the operation of the cranes is subject to the arrival and departure time of vessels.

3.2.2. Industrial electric vehicles

Industrial EVs include container tractors, reach stackers, empty handlers, trucks, and FLTs. The operation of industrial EVs depends on the operation of the corresponding crane. For example, container tractors, reach stackers, and empty handlers at the container terminal start their operation, if a crane operates. Accordingly, the power consumption of an operating industrial electric vehicle (IEV) is modelled as below:

$$P^{\mathrm{EV}_{op}}_{\mathrm{e,t}} = \sum_{v\in\Omega_v}\sum_{c\in\Omega_c}\left(\gamma^{C}_{c,v,t}\right)\mathrm{LF}^{EV}_{e}P^{\mathrm{EV}^{\max}_{op}}_{e} \tag{18}$$

The load factor LF^{EV}_{e} is utilised in this equation to consider discharging the EV battery at an average power when it is operating. Finally, $P^{\mathrm{EV}_{\max}}_{e}$ is the maximum operating power for each unit of a specific industrial EV category. The power consumption for charging industrial EVs (i.e. $P^{\mathrm{EV}_{ch}}_{\mathrm{e,t}}$) of each category is represented by (19).

$$0 \leqslant P^{\mathrm{EV}_{ch}}_{\mathrm{e,t}} \leqslant \left(\sum_{c\in\Omega_c}\sum_{v\in\Omega_v}(1-\gamma^{C}_{c,v,t})\right)P^{\mathrm{EV}^{\max}_{ch}}_{e} \tag{19}$$

This equation also shows the dependency of charging an industrial EV to the crane operation. If cranes do not operate (i.e. $\gamma^{C}_{c,v,t} = 0$) for vessel v at time t, all industrial EVs of a specific category can be charged. Based on equations (18) and (19), the state of charge of industrial EVs of a specific category can be modelled as below:

$$\mathrm{SOC}^{\mathrm{EV}}_{e,t+1} = \mathrm{SOC}^{\mathrm{EV}}_{e,t} + P^{\mathrm{EV}_{ch}}_{\mathrm{e,t}} \cdot \eta^{EV}_{e} - P^{\mathrm{EV}_{op}}_{\mathrm{e,t}} / \eta^{EV}_{e} \tag{20}$$

$$0 \leqslant \mathrm{SOC}^{\mathrm{EV}}_{e,t} \leqslant \mathrm{SOC}^{\mathrm{EV}_{\max}}_{e} \tag{21}$$

$$\mathrm{SOC}^{\mathrm{EV}}_{e,t_1} = \mathrm{SOC}^{\mathrm{EV}}_{e,t_{end}} \tag{22}$$

The state of charge of an industrial EV of a specific category is modelled by, and constrained by. In order to consider a representative day, the state of charge at the beginning and the end of each day should be equal as indicated by.

3.2.2.1. Energy storage.

Energy storage can play a vital role in electrification of ports. This technology can be utilised to store excess renewable energy generation and used when it is needed. Such capability can add a valuable flexibility to the port operation which can bring about benefits for different stakeholders. Energy storage has been considered as another asset in the port, and its operation is modelled as below (Gholami et al., 2019):

$$\mathrm{SOC}^{\mathrm{ES}}_{j,t+1} = \mathrm{SOC}^{\mathrm{ES}}_{j,t} + P^{ES_{ch}}_{j,t} \cdot \eta^{ES}_{j} - P^{ES_{dch}}_{j,t} / \eta^{ES}_{j} \tag{23}$$

$$0 \leqslant \mathrm{SOC}^{\mathrm{ES}}_{j,t} \leqslant \mathrm{SOC}^{\mathrm{ES}_{\max}}_{j} \tag{24}$$

$$0 \leqslant P^{ES_{ch}}_{j,t} \leqslant \zeta^{ES}_{j,t} \times P^{ES_{\max}}_{j} \tag{25}$$

$$0 \leqslant P^{ES_{dch}}_{j,t} \leqslant (1-\zeta^{ES}_{j,t}) \times P^{ES_{\max}}_{j} \tag{26}$$

Equation links the change of the state of charge between consecutive time steps with the charging and discharging power of the battery. Eq. (24) limits the state of charge of battery energy storage. Eqs. (25) and (26) enforce the limits on the charging and discharging power of energy storage, respectively.

3.2.2.2. Reefers.

Refrigerated containers, which are known as "reefers" are one of the main elements of port energy consumption due to their abundancy. These technologies can be considered as a potential shiftable loads in the port network, where a slight change in the temperature can have a considerable effect on the optimisation problem (Nikkhah et al., 2021). Equation relates the change of the internal temperature of the reefer with its power consumption and ambient temperature. Equation calculates the total power consumption of all reefers at Bus j of the port network. Temperature limits are enforced by, while the power consumption of the reefer is limited by.

$$\theta_{q,t+1} = \theta_{q,t} - b \cdot P^{\mathrm{Reef}}_{q,t} + a \cdot \left(\theta^{\mathrm{amb}}_{t} - \theta_{q,t}\right) \tag{27}$$

$$P^{\mathrm{Reef}}_{j,t} = \sum_{q\in\Omega_q} P^{\mathrm{Reef}}_{q,t} \tag{28}$$

$$\theta^{\min}_{q} \leqslant \theta_{q,t} \leqslant \theta^{\max}_{q} \tag{29}$$

$$0 \leqslant P_{q,t}^{\mathrm{Reef}} \leqslant P_{q}^{\mathrm{Reef}_{\max}} \tag{30}$$

4. Uncertainty modelling

Electrification of ports can present multiple risks to the electricity network. The need for providing power for berthed vessels through cold ironing could bring about potential overloading condition for the electricity network. Therefore, an optimal power management strategy is required to provide the vessel demand while considering the network limits. Under such circumstances, uncertainty associated with different inputs of such optimisation problem, especially the arrival time of vessels could bring about a considerable challenge in the decision-making process.

This paper employs a two-stage adaptive robust optimisation to deal with the possible risk of overload in electrified ports under presence of uncertainty. This method is able to provide a feasible solution for all possible realisations defined in a given uncertainty set and has multiple advantages over other uncertainty modelling techniques. Firstly, it does not require the probability distribution function of the uncertain parameters compared to stochastic programming and chance-constrained optimisation. Stochastic programming can easily become intractable when the number of scenarios increases (Sarantakos, 2022), and chance-constrained optimisation produces solutions with a given probability which might not be desirable or acceptable in a specific cases. Secondly, it is computationally tractable when used with column and constraint generation and the uncertainty set obeys specific rules. This section presents the proposed RLE method based on the formulation provided in the previous section.

To fully link the uncertainty of vessel arrival time to the shore power demand (i.e.$P_{j,t}^{D}$), this study introduces constraints (31)-(36) into the optimisation problem. Binary variable $I_{i,t}$ represents the status of load at bus i, at time step t, i.e., $I_{i,t}$ takes 1 if a vessel is at berth, otherwise it is zero. The auxiliary binary decision variable $w_{v,r}$ indicates the selected realisation r for the uncertain arrival time of vessel v and it is used to choose the worst-case realisation.

$$\sum_{r} w_{v,r} = 1 \tag{31}$$

$$\sum_{t=t_{\mathrm{arr},v}-U_{\mathrm{at}}+r-1}^{t=t_{\mathrm{arr},v}-U_{\mathrm{at}}+r-1+\mathrm{cd}_v-1} I_{\mathrm{bus}_v,t} \geqslant \mathrm{cd}_v \cdot w_{v,r}, \forall r = 1, \ldots, N_{\mathrm{r}} \tag{32}$$

$$\sum_{t \in \Omega_t} I_{\mathrm{bus}_v,t} = \mathrm{cd}_v \tag{33}$$

$$I_{\mathrm{bus}_v,t} = I_{\mathrm{bus}_c,t}, \forall t \in \Omega_t \tag{34}$$

$$I_{i,t} = 1, \forall i \notin \Omega_{\mathrm{n,sp/c}}, \forall t \in \Omega_t \tag{35}$$

$$I_{i,t} = 0, \forall i \in \Omega_{\mathrm{n,sp/c}}, \forall t \in [1, t_{\mathrm{arr},v} - U_{\mathrm{at}} - 1] \cup [t_{\mathrm{dep},v} + U_{\mathrm{at}} + 1, T] \tag{36}$$

It is assumed that the call duration of a vessel is fixed and does not depend on its arrival time. Constraint (31) ensures that only one of the uncertainty realisation intervals happens. For example, if for a vessel, there are three possible time intervals (e.g. 11:00 – 20:00, 12:00 – 21:00, and 13:00 – 22:00) which are all of the same duration (10 h), only one of the realisations can happen. Constraint (32) links decision variables $I_{i,t}$ and $w_{v,r}$, considering the call duration of vessels. Constraint (33) ensures that for the time intervals of the selected realisation, $I_{i,t}$ takes the value of one (i.e. if the first realisation is selected, $I_{i,11\text{-}20} = 1$). In (32) and (33), bus_v indicates a node of the network that supplies the shore power demand of vessel v. Constraint (34) states that if vessel v is not at berth, the corresponding crane cannot operate. Constraint (35) enforces variable $I_{i,t}$ to have the value of one for all buses which do not supply shore power demand or cranes, as their demand is not (directly) linked to a vessel being at berth. Constraint (36) ensures that shore power and crane demand is zero when a vessel is not expected to be at berth (considering uncertainty). For instance, if the arrival time of a vessel is outside 11:00 – 20:00, the uncertainty set is fixed at zero. Based on these constraints, the uncertainty set is defined as:

$$D^t(\overline{\boldsymbol{d}}^t, \widehat{\boldsymbol{d}}^t, \Gamma^t) := \left\{ \begin{array}{c} \boldsymbol{d}^t \in \mathbb{R}^{|\Omega_n|} : \sum_{i \in \Omega_n} \left(\gamma_{i,t}^{+} + \gamma_{i,t}^{-}\right) \leqslant \Gamma^t, \gamma_{i,t}^{+} + \gamma_{i,t}^{-} \leqslant 1, \gamma_{i,t}^{+}, \gamma_{i,t}^{-} \geqslant 0 \\ d_i^t = I_{i,t}\left(\overline{d}_i^t + \widehat{d}_i^t \gamma_{i,t}^{+} - \widehat{d}_i^t \gamma_{i,t}^{-}\right), \forall i \in \Omega_n \\ \boldsymbol{I} \in \Omega_{\boldsymbol{I}}\text{: } (31) - (36) \end{array} \right\} \tag{37}$$

where Γ^t is called budget of uncertainty (Bertsimas and Sim, 2004), and can be used to adjust the level of conservatism. $\Gamma^t = 0$ corresponds to the deterministic solution, and, if Γ^t takes its maximum value (equal to the number of buses of the network), the solution is fully robust, but over-conservative. The lowest Γ^t is chosen in this study which yields a zero probability of constraint violation. In (37), if a vessel has not arrived at berth, which is linked with bus i, at time t, i.e., $I_{i,t} = 0$, d_i^t is zero. The multiplication of two binary decision variables in (37) can be linearised by introducing a new binary decision variable and using the big-M method. Such linearisation will be explained in Appendix.

Based on equations (31)-(37), the compact form of the proposed two-stage adaptive robust model is shown below:

$$\min_{\boldsymbol{x}} \left(\boldsymbol{c}^{\mathrm{T}}\boldsymbol{x} + \max_{\boldsymbol{d} \in D} \min_{\boldsymbol{y} \in \Omega(\boldsymbol{x},\boldsymbol{d},\boldsymbol{I})} \boldsymbol{e}^{\mathrm{T}}\boldsymbol{y} \right) \tag{38}$$

$$\text{s.t.}$$

$$\boldsymbol{A}\boldsymbol{x} \leqslant \boldsymbol{b} \tag{39}$$

$$\Omega(\boldsymbol{x},\boldsymbol{d},\boldsymbol{I}) = \left\{ \boldsymbol{y} : \boldsymbol{H}\boldsymbol{x} + \boldsymbol{M}\boldsymbol{y} \leqslant \boldsymbol{r}, \boldsymbol{K}\boldsymbol{y} = \boldsymbol{d}, \boldsymbol{N}\boldsymbol{y} \leqslant \boldsymbol{h}, \|\boldsymbol{F}\boldsymbol{y}\|_2 \leqslant \boldsymbol{f}^{\mathrm{T}}\boldsymbol{y} \right\} \tag{40}$$

Note that the workforce cost in Equation (1) comprises of the first stage component of the objective function (i.e. $\mathbf{c}^{\mathrm{T}}\mathbf{x}$), whereas the cost of electricity and carbon emissions represents the second stage component of the objective function (i.e. $\mathbf{e}^{\mathrm{T}}\mathbf{y}$). Constraint (39) represents first stage constraints, while constraint (40) shows the second stage constraints which involve both first stage and second stage decision variables. To correctly link the second stage decision variables with new decision variables $I_{i,t}$, constraints (41) and (42) are incorporated in $\Omega(\mathbf{x},\mathbf{d},\mathbf{I})$. The following constraints state that if vessel v is not at berth at time t, all associated CHE (cranes, hoppers, and industrial EVs) do not operate.

$$P_{c,v,t}^{cr} \leqslant I_{\mathrm{bus}_c,t} \cdot P_{c}^{\max} \tag{41}$$

$$P_{\mathrm{e},t}^{\mathrm{EV}_{op}} \leqslant P_{\mathrm{e},t}^{\mathrm{EV}_{op}} = \sum_{v \in \Omega_v} \sum_{c \in \Omega_c} \left(I_{\mathrm{bus}_v,t} \gamma_{c,v,t}^{C} \right) 2\mathrm{LF}_{e}^{EV} P_{e}^{\mathrm{EV}_{op}^{\max}} \tag{42}$$

5. Solution methodology

The proposed model in Section IV-B is initially a tri-level problem. In order to improve the computational efficiency, it can be converted to a bi-level problem by dualizing the inner minimization problem and merging the second and third levels. In this study, a column and constraint generation (CCG) algorithm (Zeng and Zhao, 2013) is used, in which the resulting model is decomposed into a master problem (MP) and a subproblem (SP) which are iteratively solved until an optimality criterion is met.

5.1. Master problem

At each iteration of the algorithm, a new scenario which is obtained from the SP is added to the MP and the workforce allocation is determined in the MP considering the scenarios added so far. The MP which satisfies the constraints added up to the m^{th} iteration is shown below:

$$f_m = \min \boldsymbol{c}^T \boldsymbol{x} + \delta \tag{43}$$

$$\text{s.t. } \boldsymbol{Ax} \leqslant \boldsymbol{b} \tag{44}$$

$$\delta \geqslant \boldsymbol{e}^T \boldsymbol{y}^k, \forall k = 1, ..., m \tag{45}$$

$$\boldsymbol{Hx} + \boldsymbol{My}^k \leqslant \boldsymbol{r}, \forall k = 1, ..., m \tag{46}$$

$$\boldsymbol{Ky}^k = \boldsymbol{d}^k, \forall k = 1, ..., m \tag{47}$$

$$\boldsymbol{Ny}^k \leqslant \boldsymbol{h}, \forall k = 1, ..., m \tag{48}$$

$$\left\| \boldsymbol{Gy}^k \right\|_2 \leqslant \boldsymbol{g}^T \boldsymbol{y}^k, \forall k = 1, ..., m \tag{49}$$

where k in - represents the index of constraints and variables added to the MP up to iteration m. δ is an auxiliary variable to find the minimum cost of the second stage for all worst-case scenarios obtained from solving the previous iterations of the algorithm.

5.2. Subproblem

After solving the MP the workforce allocation (i.e. $\mathbf{x}^*$) can be obtained. For this allocation, the SP finds the worst-case realisation of uncertain parameters, which include net electricity demands and vessel arrival times.

$$\max_{\boldsymbol{d} \in D} \min_{\boldsymbol{y} \in \Omega(\boldsymbol{x}, \boldsymbol{d}, \boldsymbol{I})} \boldsymbol{e}^T \boldsymbol{y} \tag{50}$$

$$\text{s.t. } \boldsymbol{Hx}^* + \boldsymbol{My} \leqslant \boldsymbol{r}(\boldsymbol{\mu}) \tag{51}$$

$$\boldsymbol{Ky} = \boldsymbol{d}(\boldsymbol{\lambda}) \tag{52}$$

$$\boldsymbol{Ny} \leqslant \boldsymbol{h}(\boldsymbol{\pi}) \tag{53}$$

$$\|\boldsymbol{Fy}\|_2 \leqslant \boldsymbol{f}^T \boldsymbol{y}(\boldsymbol{\omega}, \boldsymbol{\varphi}) \tag{54}$$

For a given $\mathbf{d}$, the third level model becomes a second-order cone programming model. Using the conic duality theory (Ben-Tal and Nemirovski, 2001), the model can be transformed into its equivalent maximisation model, which can be merged into the second level model. By using the associated dual variables $\boldsymbol{\mu}$, $\boldsymbol{\lambda}$, $\boldsymbol{\pi}$, $\boldsymbol{\omega}$, and $\boldsymbol{\varphi}$ of the constraints, the following single-level model in (55) can be obtained. Note that since the second-order cones are self-dual, they also appear as second-order cones in the dual model. By conic duality theory (Ben-Tal and Nemirovski, 2001), the strong duality theorem holds, and therefore the primal SP and the dual SP attain the same optimal value.

$$\max_{\boldsymbol{d}, \boldsymbol{I}, \boldsymbol{\mu}, \boldsymbol{\lambda}, \boldsymbol{\pi}, \boldsymbol{\omega}, \boldsymbol{\varphi}} (\boldsymbol{r} - \boldsymbol{Hx}^*) \boldsymbol{\mu} + \boldsymbol{d\lambda} + \boldsymbol{h\pi} \tag{55}$$

$$\mathbf{M}\boldsymbol{\mu} + \mathbf{K}\boldsymbol{\lambda} + \mathbf{N}\boldsymbol{\pi} + \sum_{l=1}^{L} (\boldsymbol{F\omega} + \boldsymbol{f\varphi}) \leqslant \boldsymbol{e} \tag{56}$$

$$\|\boldsymbol{\omega}\|_2 \leqslant \boldsymbol{\varphi} \tag{57}$$

where L is the number of constraints in. The single-level problem is nonlinear due to the multiplication of variables $\mathbf{d}$ and $\boldsymbol{\lambda}$. The linearisation of this model is explained in Appendix.

After linearising the model, it becomes a mixed-integer second-order cone programming problem, which can be solved by commercial solvers, such as Gurobi (Gurobi, 2024). Algorithm 1 (Sarantakos, 2022) shows the procedure of the aforementioned solution methodology.

Algorithm 1: Column and Constraint Generation

1. Set LB = -∞, UB = +∞, $m = 0$, tolerance ε.
2. **while** (UB - LB < ε) **do**

(*continued on next column*)

(*continued*)

Algorithm 1: Column and Constraint Generation

3. Solve the MP -. Get optimal solution and objective, $\mathbf{x}^*$ and f_m, respectively.
   LB ← max{LB, f_m }.
4. Given $\mathbf{x}^*$, solve the dual SP -. Get worst-case uncertainty realization $\mathbf{d}^*$ and objective f_s.
   UB ← min{UB, $\mathbf{c}^T\mathbf{x}^* + f_s$ }.
5. $\mathbf{d}^{m+1} \leftarrow \mathbf{d}^*$. Introduce new variables $\mathbf{y}^{m+1}$. Add constraints - to the MP.
6. $m \leftarrow m + 1$.
7. **end**
8. Return $\mathbf{x}^*$.

6. Case Study: Port of Tyne

6.1. Overview

For a representative case study, a medium sized multipurpose UK port is selected as a test bed for the proposed model. PoT is positioned in the middle of the UK's 51 'major' ports (defined as handling over 1 M tonnes of cargo per year and/or strategically important (Transport, 2021), in terms of size and cargo throughput. Like many medium sized ports, PoT handles a diverse cargo mix including dry, bulk, roll on/roll off (RoRo), breakbulk/general cargo, and containerised cargoes. Each of these cargoes, which have different characteristics, is transported by different types of ships and requires specific CHE for vessel loading/unloading and handling within the port.

6.2. Data processing

The operational data for the PoT is collected at different stages. The port comprises four berths, each identified by its corresponding vessel types and the cargoes handled at each berth. These berths include: 1) container ships, 2) bulk carriers transporting biomass, 3) multipurpose/general cargo ships carrying palletised plywood, and 4) RoRo ships, specifically car carriers. These represent the primary cargo handling operations at the port and enable the modelling of demands for various electrified CHE and shore power. Table 2 summarizes the information on each berth based on vessel types and the cargoes handled at each berth.

At the second stage, based on information obtained about each berth (Table 2), the type and number of CHE assets required to unload each ship type have been ascertained. This information is obtained from the results of interviews with operational managers of the PoT. The cargo handling process, number of CHE assets required for each berth, and the staff required for operation of each asset are summarised in Table 3. The information provided in this table is utilised as an input for the number of assets and the workforce cost in problem formulation (Section 2). The operational processes that follow the arrival of each vessel type are explained in Section 2. The detailed explanation about data acquisition is given in Reference (Sarantakos, 2023).

PoT's electricity network is a medium-voltage grid which supplies different sites. The diagram of this network is shown in Fig. 3, which has been extended to include future assets (energy storage, a large-scale

Table 2
Terminals, berths, ships, and cargo types modelled in the case study.

Terminal	No. of berths included in case study	Ship type considered in case study	Shoreside cargo handling operation
Tyne Car Terminal	2	Car carrier	Vehicles
Tyne Bulk Terminal	1	Bulk carrier	Biomass
Container Terminal	1	Containership	Containers
General Cargo Terminal	1	Bulk carrier/general cargo	Plywood

Table 3
Process modelled, and workforce/equipment used for each type of cargo.

Terminal	Process	No. of assets	Workforce (Number of staff allocated)
Container Terminal	Vessel & CHE operation for container import/export	1x shore power	–
		2x ship to shore cranes	1/operating crane (max. 2)
		12x container tractors	3/operating crane (max. 6)
		4x reach stackers	1/operating crane (max. 2)
		4x empty handlers	1/operating crane (max. 2)
Bulk Terminal	Vessel & CHE operation for biomass import	1x shore power	–
		2x cranes	1/operating crane (max. 2)
		2x hoppers	1/operating crane (max. 2)
		12x trucks	3/operating crane (max. 6)
General Cargo Terminal 1	Vessel & CHE operation for plywood import	1x shore power	–
		2x cranes	1/operating crane (max. 2)
		20x forklift trucks (FLTs)	5/operating crane (max. 10)
Car Terminal	Vessels only	2x shore power	–

solar PV installation, shore power, and a fully electrified CHE fleet). Existing loads (buildings, reefer containers, CHE that is already electrified) are also shown. In Fig. 3, the branch shown in red is at a high risk of overload due to the additional demand from electrification. At present, the port's CHE includes both electric and diesel-powered assets. As part of its future strategy, the port intends to become an all electric port for the assets it owns, which include most of the CHE detailed in Table 3. Electrification of some of this diesel-powered CHE is already underway, while the port is also proceeding with a significant solar PV installation, while also considering shore power supplies for some of its berths. This provides a valuable real-world opportunity for investigating the modelling and scheduling of electrified CHE and its impact on the electricity network, and for examining the impact of neglecting uncertainty on electrified port operation.

An important factor in defining the port consumption is the time period a ship would be at berth, as the operation of CHE assets depends on the availability of vessels. Having such data, the starting point of different assets operation along with their power consumption could be defined. This was achieved through analysing the vessel call data from the vessel traffic service for a period of 9 months during 2020–2021, and obtaining a daily average for the purpose of the simulation in this paper. Table 4 shows the time plan of the five vessels considered in this case study. Time steps shaded in blue correspond to the expected call of each vessel e.g., vessel V1 is expected to arrive at time step 12 and depart at time step 21. Time steps in light blue indicate that vessels can arrive up to two hours earlier or later. It is assumed that the call duration of each vessel is fixed, i.e., if V1 arrives at time step 11, it will depart at time step 20, and if it arrives at time step 13, it will depart at time step 22. Table 5 shows the possible realisations for vessel V1. Table 6 presents the call duration and shore power demand of each vessel.

The other key parameter values used in the simulation are presented in Table 7. The electricity price and grid carbon intensity for a day are shown in Fig. 4.

7. Results

The proposed methodology was applied to the PoT as the case study with the details provided in the previous section. The optimisation model was implemented in MATLAB R2017a with the aid of YALMIP (Lofberg, 2004) and solved using Gurobi (Gurobi, 2024). An Intel Core

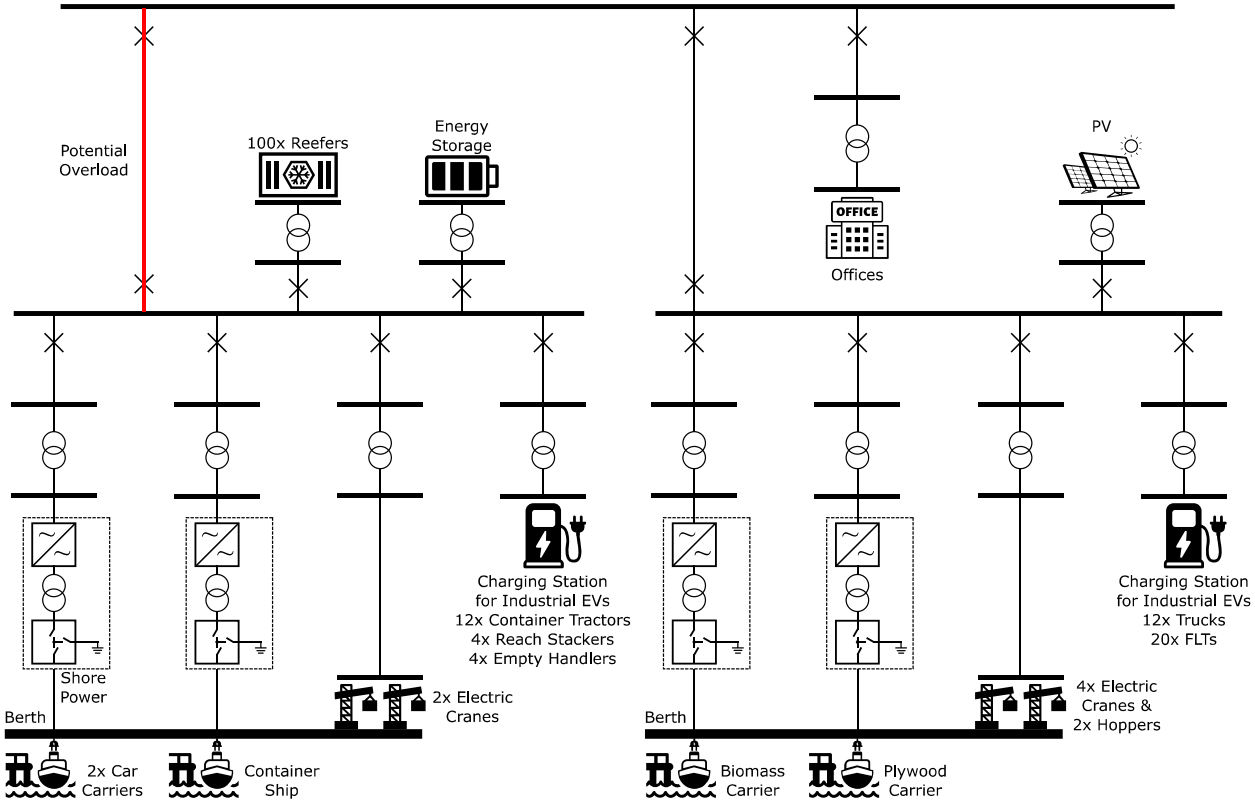

Fig. 3. Case study port network showing all existing and future loads (shore power, CHE, reefers, and offices).

Table 4
Vessels Time Plan.

	1	2	3	4	5	6	7	8	9	10	11	12	13	14	15	16	17	18	19	20	21	22	23	24
V1																								
V2																								
V3																								
V4																								
V5																								

V1: Car Carrier 1, V2: Car Carrier 2, V3: Container Ship, V4: Bulk Carrier 1 (Biomass), V5: Bulk Carrier 2. (Plywood).

Table 5
Possible Realisations for Vessel V1.

	1	2	3	4	5	6	7	8	9	10	11	12	13	14	15	16	17	18	19	20	21	22	23	24
r1																								
r2																								
r3																								
r4																								
r5																								

Table 6
Call Duration and Shore Power Demand of each Vessel.

Vessel	Berth	Call Duration	Shore Power Demand
Car Carrier 1 (V1)	TCT1	10 h	1 MW
Car Carrier 2 (V2)	TCT2	9 h	1 MW
Container Ship (V3)	Container terminal	8 h	500 kW
Biomass Carrier (V4)	TBT	15 h	300 kW
Plywood Carrier (V5)	General cargo terminal	10 h	200 kW

Table 7
Key parameters used in the simulation.

Parameter	Value
Max. average crane power during an hourly period	82.2 kW (Zhao et al., 2016)
Hopper average power	55.5 kW (Sarantakos, et al., 2023)
Reefer max. power	5.7 kW (Kanellos et al., 2019)
Reefer temp. range	−29 °C ± 1 °C (Kanellos et al., 2019)
Reefer parameter *a*	2.9035 × 10^{-3} (Kanellos et al., 2019)
Reefer parameter *b*	0.0537 °C/kW (Kanellos et al., 2019)
CHE load factors	≈0.5 (Starcrest Consulting Group, 2007)
Carbon price (4 Feb 22)	87.92 £/tonne (Carbon price, 2024)
PV	752 kW (Ninja, 2024)
Energy storage	0.5 MW / 1 MWh
Container tractors	100 kW / 200 kWh (Container tractor, 2024
Reach stackers	100 kW / 200 kWh (ERS, 2024)
Empty handlers	100 kW / 200 kWh (EEH, 2024)
Trucks	100 kW / 200 kWh (Electric Truck, 2024)
FLTs	33 kW / 66 kWh (Electric Forklift, 2024)
Efficiency (η) for storage and industrial EVs	0.95 (e.g. (EEH, 2024)
Workforce cost	50 £/person-hour

i7 octa-core processor at 3.0 GHz with 32 GB of RAM was used for the simulations. Optimality gap was set to 1 %. This section presents the simulation results for the proposed RLE model. The efficiency of this method is benchmarked against several case studies, presented below:

Case I: Logistic-only model. This case study solves the model without consideration for the port power network constraints (i.e. neglecting constraints (2)-(11)).

Case II: Deterministic model. This case study solved the model without consideration for uncertainty in the input data. This case study is compared against Case I to demonstrate the necessity of considering a joint logistic-electric model.

Case III: The proposed RLE model. This is the main case study, which considers a logistic-electric model and accounts for uncertainty of input data. This case study is compared with Case II so as to investigate the effect of uncertainty on the decision making of all electric ports.

The computational efficiency of the proposed method is confirmed by Table 8, which shows the relaxation gap of the proposed model. This relaxation gap corresponds to the original constraints (6), which is defined as below:

$$Gap_{ij,t} = \left| \sqrt{L_{ij,t}} - \sqrt{\left(P_{ij,t}^2 + Q_{ij,t}^2\right) \Big/ u_{i,t}} \right| \tag{58}$$

The mean value of this gap and the mean value of the current (squared root of $L_{ij,t}$) are shown in Table 8. The comparison of these two values (4 orders of magnitude) demonstrates satisfactory accuracy of the model.

7.1. CO_2 equivalent emissions

Neglecting the uncertainty in the arrival time of vessels can have environmental and economic repercussions. If a ship arrives at the port but cannot connect to shore power because the port's network is already at capacity, it is compelled to operate its auxiliary engines while berthed. For example, in Table 4, if vessel V1 arrives one hour late due to the uncertainty in its arrival (e.g. time periods 10 and 11), it needs to burn marine gas oil (MGO) in its auxiliary engines instead of being supplied by shore power.

To illustrate the impact of uncertainty on ship emissions, the hourly CO2 equivalent emissions resulting from the combustion of marine gas oil (MGO) in a ship's auxiliary engines are contrasted with the emissions during the same hours when the ships are connected to shore power. The data used for this comparison is derived from the actual engine data of the vessels detailed in Tables 2 and 3. For each berth, all the ships from the call data were listed, and the individual hourly emissions of Carbon Dioxide (CO2), Methane (CH4), and Nitrous Oxide (N2O) of each ship were calculated and then averaged for all the ships at that berth. The hourly averages of the individual greenhouse gases (CO2, CH4, and N2O) were then converted to CO2 equivalent emissions.

Uncertainty in arrival time of vessels (see Table 4) can result in the delay of connecting the ships to shore power. The hourly CO2 equivalent emissions of these ships at berth when burning MGO in auxiliary engines while waiting to be served, and connected to shore power is shown in Fig. 5. This figure shows a minimum of 150 % increase in CO2 equivalent emissions when ships use their auxiliary engines compared to the case they are connected to the shore power. It is noteworthy that the

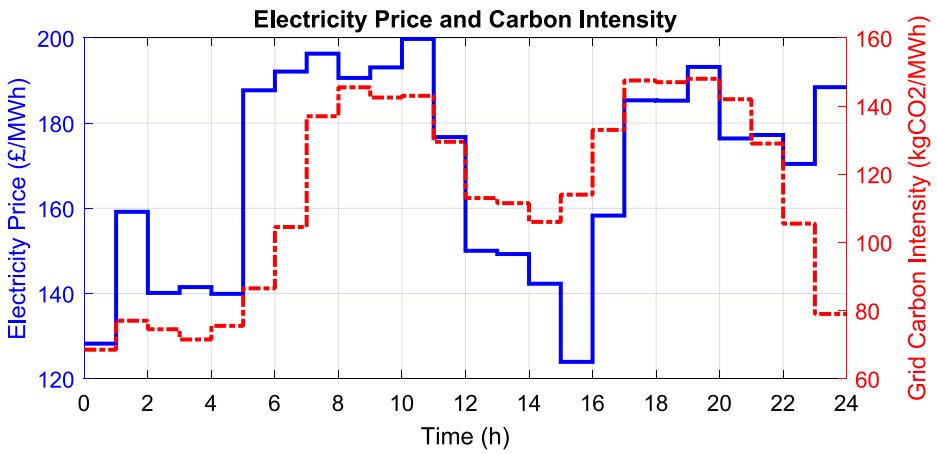

Fig. 4. Electricity price and grid carbon intensity for a day (in February 2022) (Carbon intensity, 2024; Elexon, 2024).

Table 8
Relaxation Gap for the proposed optimisation.

Relaxation Gap	Mean Value	Variable	Mean Value	Relative Gap
Gap (A)	1.62×10^{-3}	$L_{ij,t}^{0.5}$ (A)	12.21	1.33×10^{-4}

evaluation of environmental impact centres around quantifying the greenhouse gas emissions released from burning MGO.

As well as greenhouse gases, the combustion of MGO in auxiliary engines also results in the release of air quality pollutants such as carbon monoxide, particulate matter, nitrogen oxides, sulphur oxides, and non-methane volatile organic compounds. On their release, these toxic compounds pollute the local air and environment, causing ecological damage and harm to human health. In contrast to the global impact of greenhouse gases, the effects of air pollutants occur in the immediate vicinity of their release and are therefore of high concern to ports located at or near urban centres. Connecting to shore power enables ships' auxiliary engines to be switched off, virtually eliminating air pollutant emissions. This improves the air quality around the port and reduces the impact of port operations on the local environment and residents. Noise and vibration are also reduced, which improves the working environment for crew and port operatives.

Although the assessment of environmental impact focuses on quantifying the greenhouse gases emitted by vessels utilizing their auxiliary engines instead of receiving shore power, in future work the analysis could be extended to include air quality pollutant emissions.

In addition to emission and the risk of network overload, uncertainty can generate different expenses (e.g. demurrage charges, and network reinforcement) to the port operators and ship owners. Therefore, considering the uncertainty associated with operation of electrified ports is an important factor that should be considered in their optimal management.

7.2. Logistics-only model

Fig. 6 shows the loading of branch 1, when the electricity network equations are not considered. As can be seen in this figure, branch 1 experienced an overload during 15:00 – 16:00, when electricity price takes its lowest value (see Fig. 4), resulting in an increase for power demand from the flexible assets. Note that this overload occurred even without considering the impact of uncertainty. As can be seen in Fig. 7, however, solving the model for a joint logistics-electric optimisation has resulted in no overload in the branch. Comparison of these figures clearly demonstrates the needs for a joint logistics-electric model in optimising power management of all electric ports. This case studies are solved based on the solution methodology described in Section 4.

7.3. Deterministic model

In Fig. 7, it can be observed that the margin between the branch loading during 15:00–16:00 is in its maximum value, which can present a high risk of violation due to the sudden changes in the operation of the network. This sudden change can happen due to the uncertainty in the arrival time of a vessel. To demonstrate the risk involved in the deterministic solution, which neglects uncertainty in the vessel arrival time,

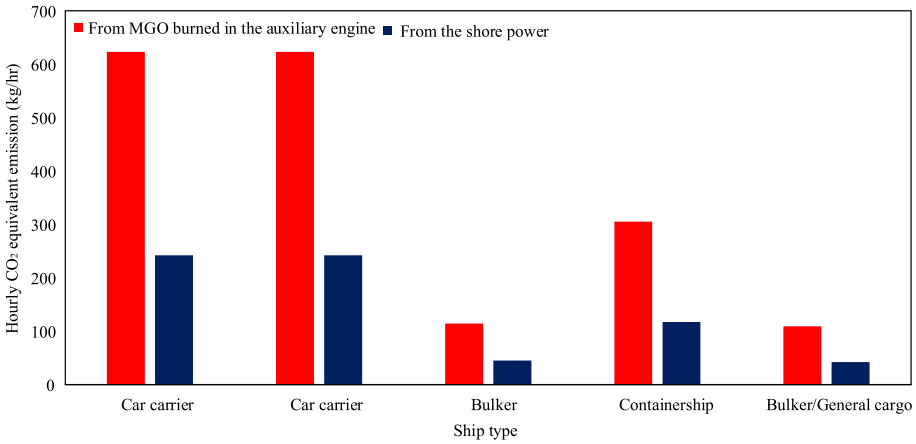

Fig. 5. Average hourly CO_2 equivalent emissions from MGO burned in auxiliary engines and shore power.

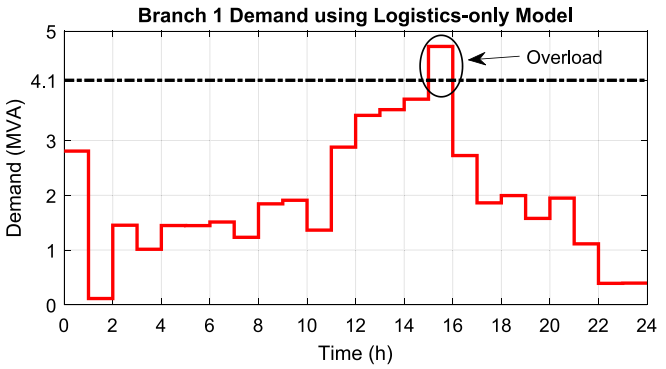

Fig. 6. Power demand of branch 1 for Case I: the use of a logistics-only model led to an overload in this case study.

network demand, and renewable power generation, the Monte Carlo simulation is utilised here. To do so, the proposed model in Case II is solved for 100 iterations of Monte Carlo simulation, with consideration for variation in the vessel arrival time, network demand, and renewable power generation. Fig. 8 shows the corresponding results for ± 2 h vessel arrival time uncertainty and ± 20 % for net demand. Each colour in this figure represents one iteration of 100 Monte Carlo simulation. The variation of these iterations is more obvious in peak hours (e.g. time period between 12 and 16). The line limit represents the maximum amount of power which can be transferred through branch 1 (Fig. 3) without exceeding voltage limits of the transformer. The resulting probability of constraint violation (PoCV) is equal to 70 %, meaning that there is a network thermal limit violation for at least one hour in 70 % of the simulated days. This PoCV is justified by the departure of vessel V2 at time step 14 and the arrival of vessel V3 at time step 15. This means that an overlap of shore power demands of these two vessels is possible (at time steps 13–16, or 12:00 – 16:00), if uncertainty is considered (see Table 4). Moreover, electricity price at time step 16 is the lowest throughout the day (see Fig. 4), which encourages an increase in the consumption of flexible devices (reefers, CHE, and storage charging).

Table 9 compares the proposed RLE with the proposed berth allocation in Reference (Sun et al., 2022). It is shown in this contemporary study the optimal berth allocation based on vessel arrival can result in 4.8 % cost saving. Comparing the proposed method in this paper with such state-of-the-art studies allows us to investigate the importance of uncertainty in arrival time of vessels and its effect on probability of constraint violation. It is shown that the formulation proposed in (Sun et al., 2022) cannot provide a feasible solution when uncertainty is considered. This means that vessels arriving at the port might need to

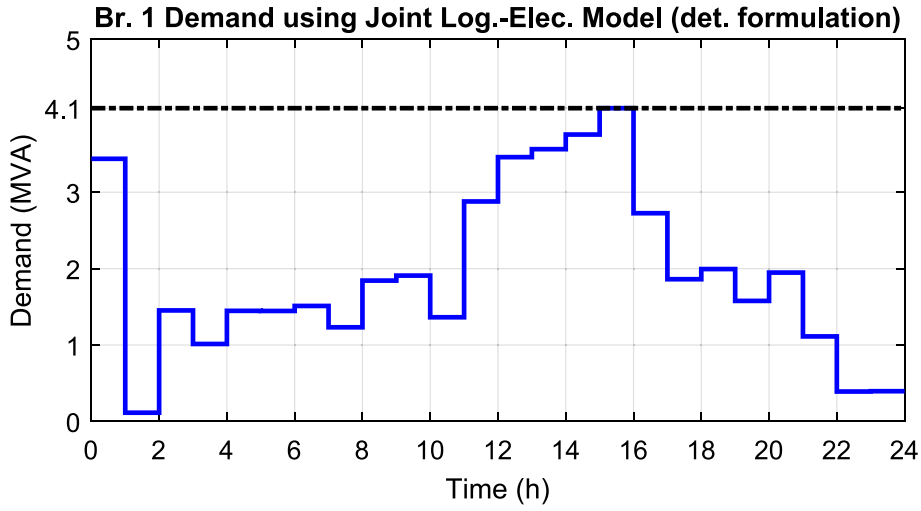

Fig. 7. Power demand of branch 1 for Case II: using the proposed joint logistics-electric optimisation model.

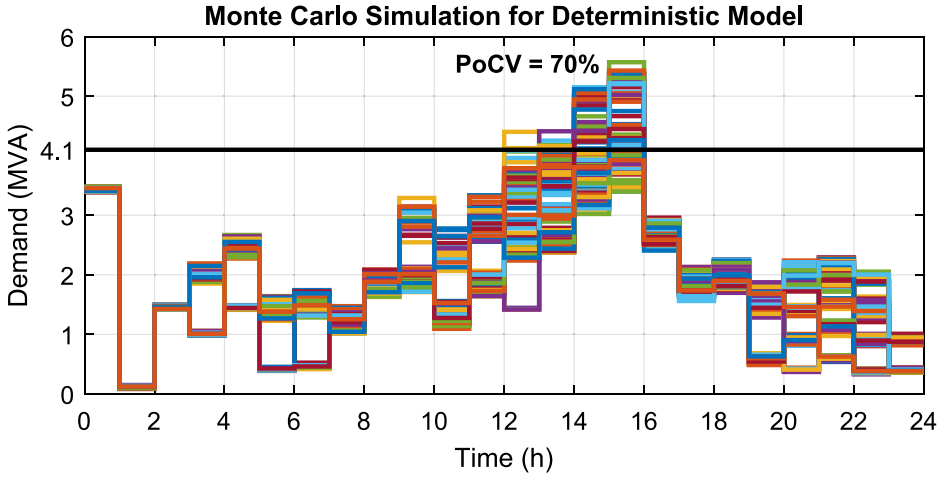

Fig. 8. 100 Monte Carlo simulations to investigate the feasibility of the schedule produced by the deterministic model in Case II. An overload occurred in 70% of the simulated days. The black line represents the line limit.

Table 9
PoCV, Robust Optimal Value, and Mean Objective Function Value for the two models.

Model	PoCV	Rob. Opt. Value	(Mean) Obj. Fun. Value
(Sun et al., 2022)	70 %	–	£18,723
Proposed	0 %	£19,606 (+4.7 %)	£18,786 (+0.3 %)

wait at anchorage to prevent a network overload in the case that another vessel is delayed in the port. It should be noted that extended vessel waiting times will lead to increased carbon emissions. Although the value of the objective function for the deterministic formulation is £18,723, the corresponding PoCV is 70 %, which presents an unacceptable risk to the port's operation. However, the optimal value of the cost in the RLE is £19,606 (i.e. + 4.7 % increase compared to the deterministic case). The average cost (over 100 Monte Carlo simulations) of the proposed model is £18,786 which is only + 0.3 % more than the deterministic case. This means that for only + 0.3 % increase in the cost, a feasible solution for all uncertainty realisations can be achieved.

The results obtained in Fig. 8 (e.g. having a PoCV as high as 70 %) demonstrate the needs for considering the uncertainty of input data including the vessel arrival time in optimal management of port operation. Therefore, the proposed RLE model in Case III proposes a robust framework which considers a conservative margin to protect the network from an overload even when the worst-case scenario is realised.

7.4. Robust model

Fig. 9 illustrates the results of the Monte Carlo simulation of the proposed RLE model in Case III. In this simulation, first stage variables are considered fixed, whereas second stage variables are adjustable to each uncertainty realization. As can be seen in Fig. 9, PoCV is zero, demonstrating the effectiveness of the proposed method compared to the deterministic case (i.e. Case II). Fig. 10 shows the power consumption of reefers in Case III for each Monte Carlo simulation. As can be seen in this figure, reefer demand is adjusted to each uncertainty realization to avoid the overload (because of the potential overlap of shore power demands of vessels V2 and V3). Reefer demand is then increased during 16:00 – 17:00 compared to the deterministic model following the initial reduction during 12:00 – 16:00 so as to compensate the temperature rise due to the reduced cooling. The results obtained in Fig. 10 indicate the significance of flexible assets in the port, where the reefers power consumption is adjusted in order to avoid PoVC (i.e. increasing the robustness in face of uncertainty in the vessel arrival time).

Fig. 11 shows the charging power of the energy storage at the port for each Monte Carlo simulation. It can be observed that charging power is adjusted to accommodate the line limit during time steps 13–16 (i.e., 12:00 – 16:00), at which there is a probability of an overlap in shore power demand of vessels V2 and V3. There is an increase in the charging power of the energy storage during 12:00 – 14:00 (time steps 13 and 14) and 16:00 – 17:00 (time step 17), while it experienced a reduction during 14:00 – 16:00 (time steps 15 and 16) compared to the deterministic model. The changes in the energy storage as another flexible asset in the port operation, highlights the importance of these technologies in improving robustness in face of uncertainty in the arrival time of vessels.

Supply disruption events along global supply chains, such as the recent impact of Brexit on the UK, can significantly influence the optimal operation of ports. The uncertainty in the supply chain extends beyond berth allocation and can have a substantial effect on the planning of all-electric ports. An effective method for assessing supply disruptions along global supply chains is detailed in (Berr et al., 2023 Nov 13). This aspect could be considered as a future research direction.

8. Conclusion

This paper presents a joint logistics-electric framework for the optimal operation of electrified ports with the aim of minimising the total cost of energy, carbon emissions, and workforce. This framework ensures network constraints are not violated in the presence of uncertainties from electricity demand, renewable power generation, and vessel arrival time. Shore power and electrification of cargo handling equipment for a range of vessel types is modelled within the present framework. Deterministic formulations in existing literature are proved to be ineffective, as they can result in a high probability of constraint violation (e.g., 70 % for the case study presented in this paper). A two-stage adaptive robust model is proposed in this paper which can ensure a feasible solution (i.e., zero probability of a network constraint violation) for all uncertainty realisations defined in a specific uncertainty set with only + 0.3 % increase in average operation cost and + 4.7 % in the worst-case scenario. These results demonstrate the advantages of the proposed method for the optimal operation of electrified ports under uncertainty.

This study primarily explored the impact of uncertainty on optimal power management and the likelihood of electricity network power flow constraint violations in ports. Several potential limitations pave the way for future research directions. Firstly, it would be valuable to delve into important economic considerations, such as demurrage charges, stemming from uncertainties in vessel arrival times. This uncertainty could also extend to influencing network reinforcement during the planning phase. Secondly, the examination of a two-hour time window of uncertainty in vessel call duration could benefit from a more in-depth

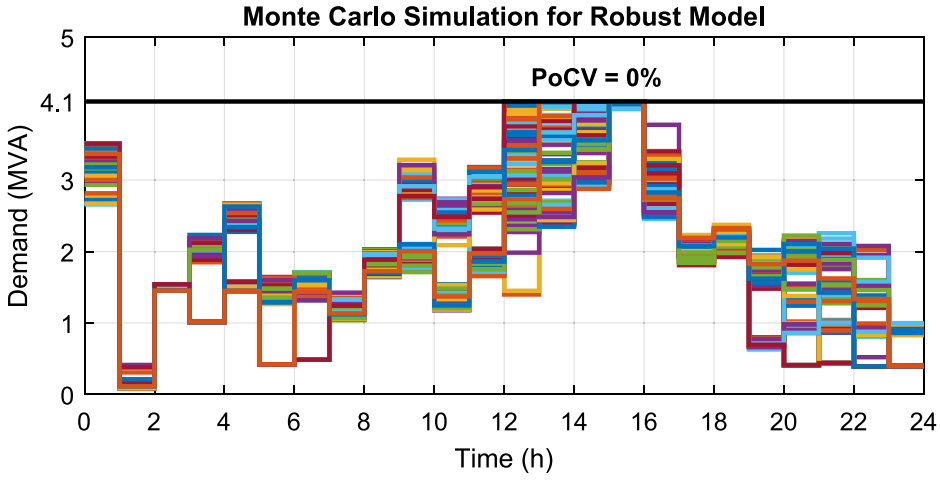

Fig. 9. Monte Carlo simulation for the robust model in Case III.

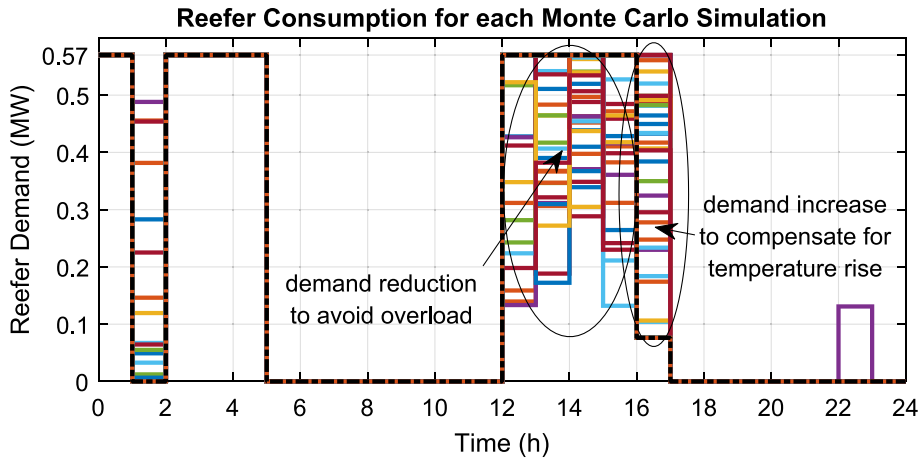

Fig. 10. Reefer power demand for each Monte Carlo simulation. Dash-dotted black lines correspond to the deterministic model.

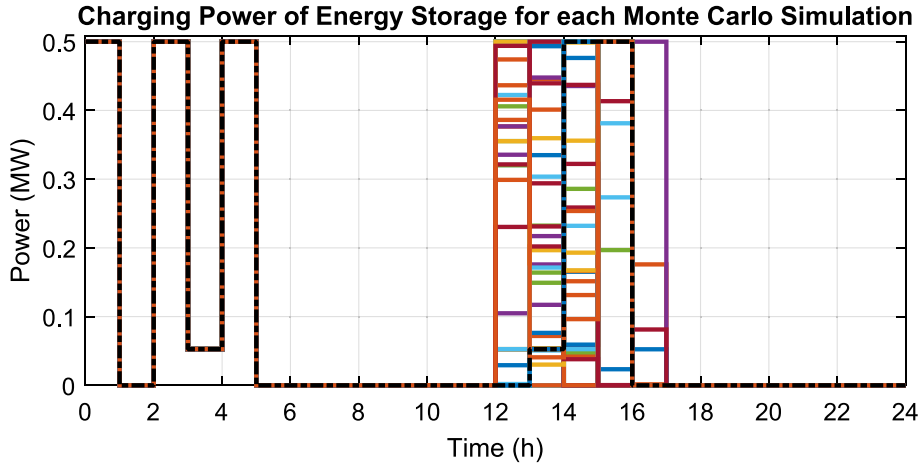

Fig. 11. Charging power of energy storage for each Monte Carlo simulation. The dash-dotted black line corresponds to the deterministic model.

exploration of variations due to various port operation policies. Finally, the influence of uncertainty along global supply chains reaches beyond berth allocation, impacting the optimal operation and planning of ports. Consequently, recognizing its significance, this aspect has been identified as a prospective area for future research to expand upon the findings presented in this paper.

CRediT authorship contribution statement

Ilias Sarantakos: . **Saman Nikkhah:** Formal analysis, Validation, Visualization, Writing – review & editing. **Meltem Peker:** Conceptualization, Methodology, Visualization, Writing – review & editing. **Annabel Bowkett:** . **Timur Sayfutdinov:** Formal analysis, Funding acquisition, Writing – review & editing. **Arman Alahyari:** Formal analysis, Methodology, Software, Writing – review & editing. **Charalampos Patsios:** Funding acquisition, Investigation, Project administration, Resources, Supervision, Writing – review & editing. **John Mangan:** Funding acquisition, Investigation, Resources, Supervision, Writing – review & editing. **Adib Allahham:** Conceptualization, Formal analysis, Funding acquisition, Writing – review & editing. **Eleni Bougioukou:** Formal analysis, Funding acquisition, Writing – review & editing. **Alan Murphy:** Funding acquisition, Investigation, Resources, Supervision, Writing – review & editing. **Kayvan Pazouki:** .

Declaration of competing interest

The authors declare that they have no known competing financial interests or personal relationships that could have appeared to influence the work reported in this paper.

Data availability

Data will be made available on request.

Appendix

The nonlinear single-level problem can be linearised by adding new decision variables $\mathbf{q}$, $\mathbf{z}^{+}$, and $\mathbf{z}^{-}$ and using the big-M linearization technique. Based on Constraint (37), $\mathbf{d}$ can be defines as:

$$\boldsymbol{d} = \boldsymbol{I}(\bar{\boldsymbol{d}} + \widehat{\boldsymbol{d\gamma}}^{+} - \widehat{\boldsymbol{d\gamma}}^{-}) \tag{A1}$$

Therefore, $\mathbf{d\lambda}$ is equal to:

$$d\lambda = I(\bar{d} + \widehat{d\gamma}^{+} - \widehat{d\gamma}^{-})\lambda \tag{A2}$$

Defining new decision variables $\mathbf{q}$, $\mathbf{z}^{+}$, and $\mathbf{z}^{-}$ as follows:

$$q = I\lambda \tag{A3}$$

$$z^{+} = q\gamma^{+} \tag{A4}$$

$$z^{-} = q\gamma^{-} \tag{A5}$$

The following equation can be obtained:

$$d\lambda = (\bar{d} + \widehat{d\gamma}^{+} - \widehat{d\gamma}^{-})\underbrace{I\lambda}_{q} = \bar{d}q + \hat{d}\underbrace{\gamma^{+}q}_{z^{+}} - \hat{d}\underbrace{\gamma^{-}q}_{z^{-}} = \bar{d}q + \widehat{dz}^{+} - \widehat{dz}^{-} \tag{A6}$$

which is linear, and the new decision variables $\mathbf{q}$, $\mathbf{z}^{+}$, and $\mathbf{z}^{-}$ are constrained as follows:

$$-M(1-I) + \lambda \leqslant q \leqslant \lambda + M(1-I) \tag{A7}$$

$$-MI \leqslant q \leqslant MI \tag{A8}$$

$$-M(1-\gamma^{+}) + q \leqslant z^{+} \leqslant q + M(1-\gamma^{+}) \tag{A9}$$

$$-M\gamma^{+} \leqslant z^{+} \leqslant M\gamma^{+} \tag{A10}$$

$$-M(1-\gamma^{-}) + q \leqslant z^{-} \leqslant q + M(1-\gamma^{-}) \tag{A11}$$

$$-M\gamma^{-} \leqslant z^{-} \leqslant M\gamma^{-} \tag{A12}$$

where $\mathbf{M}$ are sufficiently large numbers.

References

Agra, A., Oliveira, M., 2018. MIP approaches for the integrated berth allocation and quay crane assignment and scheduling problem. European Journal of Operational Research. https://doi.org/10.1016/j.ejor.2017.05.040.

Baran, M.E., Wu, F.F., Apr. 1989. Network reconfiguration in distribution systems for loss reduction and load balancing. IEEE Trans. Power Del. 4 (2), 1401–1407. https://doi.org/10.1109/61.25627.

Ben-Tal, A., Nemirovski, A., 2001. Lectures on Modern Convex Optimization. SIAM, Philadelphia, PA, USA.

Berr, M., Hischier, R., Wäger, P., 2023 Nov 13. Assessing Short-Term Supply Disruption Impacts within Life Cycle Sustainability Assessment— A Case Study of Electric Vehicles. Environmental Science & Technology.

Bertsimas, D., Sim, M., 2004. The Price of Robustness. Oper. Res. 52 (1), 35–53. https://doi.org/10.1287/opre.1030.0065.

Bierwirth, C., Meisel, F., 2015. A follow-up survey of berth allocation and quay crane scheduling problems in container terminals. European Journal of Operational Research 244 (3), 675–689. https://doi.org/10.1016/j.ejor.2014.12.030.

"Carbon Intensity." https://carbonintensity.org.uk/ (accessed.

"Carbon Price." https://ember-climate.org/data/data-tools/carbon-price-viewer/ (accessed.

Connected Places Catapult, "(Confidential)," 2021.

Chua, Y.J., Soudagar, I., Ng, S.H., Meng, Q., 2023. Impact analysis of environmental policies on shipping fleet planning under demand uncertainty. Transportation Research Part d: Transport and Environment 120, 103744.

"Container Tractor." https://www.terbergspecialvehicles.com/en/vehicles/terminal-tractors/ (accessed.

Department for Transport, "Clean Maritime Plan," UK, 2019. [Online]. Available: https://assets.publishing.service.gov.uk/government/uploads/system/uploads/attachment_data/file/815664/clean-maritime-plan.pdf.

Dulebenets, M.A., 2022. Multi-objective collaborative agreements amongst shipping lines and marine terminal operators for sustainable and environmental-friendly ship schedule design. Journal of Cleaner Production. 15 (342), 130897.

"Electric Empty Handler." https://www.kalmarglobal.com/equipment-services/masted-container-handlers/electric-empty-handler-ECG70/ (accessed.

"Electric Forklift." https://toyota-forklifts.co.uk/our-products/electric-counterbalanced-trucks/80-volt/toyota-traigo-80-electric-forklift-5t/ (accessed.

"Electric Truck." https://www.volvotrucks.com/en-en/trucks/trucks/volvo-fh/volvo-fh-electric.html (accessed.

Elexon. "Price Profiles." https://www.bmreports.com/bmrs/?q=balancing/marketindex (accessed.

"Electric Reach Stacker." https://www.kalmarglobal.com/equipment-services/reachstackers/electric-reachstacker/ (accessed.

Fang, S., Wang, Y., Gou, B., Xu, Y., 2020. Toward Future Green Maritime Transportation: An Overview of Seaport Microgrids and Electrified Ships. IEEE Trans. Veh. Technol. 69 (1), 207–219. https://doi.org/10.1109/TVT.2019.2950538.

Farivar, M., Low, S.H., 2013. Branch Flow Model: Relaxations and Convexification—Part I. IEEE Trans. Power Syst. 28 (3), 2554–2564. https://doi.org/10.1109/TPWRS.2013.2255317.

Frontier Economics, "Reducing the UK Maritime Sector's Contribution to Air Pollution and Climate Change: Potential Demands on the UK Energy System from Port and Shipping Electrification - A Report for the Department for Transport," 2019.

Gholami, A., Shekari, T., Grijalva, S., 2019. Proactive Management of Microgrids for Resiliency Enhancement: An Adaptive Robust Approach. IEEE Trans. Sustain. Energy 10 (1), 470–480. https://doi.org/10.1109/TSTE.2017.2740433.

Giallombardo, G., Moccia, L., Salani, M., Vacca, I., 2010. Modeling and solving the Tactical Berth Allocation Problem. Transportation Research Part b: Methodological 44 (2), 232–245. https://doi.org/10.1016/j.trb.2009.07.003.

Gurobi Optimization. http://www.gurobi.com (accessed.

He, J., Huang, Y., Yan, W., Wang, S., 2015. Integrated internal truck, yard crane and quay crane scheduling in a container terminal considering energy consumption. Expert Systems with Applications 42 (5), 2464–2487. https://doi.org/10.1016/j.eswa.2014.11.016.

Hu, Q.-M., Hu, Z.-H., Du, Y., 2014. Berth and quay-crane allocation problem considering fuel consumption and emissions from vessels. Computers & Industrial Engineering 70, 1–10. https://doi.org/10.1016/j.cie.2014.01.003.

International Maritime Organisation, "Fourth IMO GHG Study,", 2020. [online]. Available. https://www.imo.org/en/OurWork/Environment/Pages/Fourth-IMO-Greenhouse-Gas-Study-2020.aspx.

Iris, Ç., Lam, J.S.L., 2019. A review of energy efficiency in ports: Operational strategies, technologies and energy management systems. Renewable and Sustainable Energy Reviews 112, 170–182. https://doi.org/10.1016/j.rser.2019.04.069.

Kanellos, F.D., Volanis, E.M., Hatziargyriou, N.D., 2019. Power Management Method for Large Ports With Multi-Agent Systems. IEEE Trans. Smart Grid 10 (2), 1259–1268. https://doi.org/10.1109/TSG.2017.2762001.

Kenan, N., Jebali, A., Diabat, A., 2022. The integrated quay crane assignment and scheduling problems with carbon emissions considerations. Computers & Industrial Engineering 165, 107734. https://doi.org/10.1016/j.cie.2021.107734.

Liu, D., Ge, Y.-E., 2018. Modeling assignment of quay cranes using queueing theory for minimizing CO2 emission at a container terminal. Transp. Res. Part d: Transp. Environ. 61, 140–151. https://doi.org/10.1016/j.trd.2017.06.006.

Liu, C., Xiang, X., Zheng, L., 2017. Two decision models for berth allocation problem under uncertainty considering service level. Flexible Services and Manufacturing Journal 29 (3), 312–344. https://doi.org/10.1007/s10696-017-9295-5.

Lofberg, J., 2004. "YALMIP : a toolbox for modeling and optimization in MATLAB," in. IEEE International Conference on Robotics and Automation 2004, 284–289. https://doi.org/10.1109/CACSD.2004.1393890.

Nguyen, P.-N., Woo, S.-H., Kim, H., 2022. Ship emissions in hotelling phase and loading/unloading in Southeast Asia ports. Transportation Research Part d: Transport and Environment 105, 103223.

Nikkhah, S., Allahham, A., Royapoor, M., Bialek, J.W., Giaouris, D., 2021. Optimising building-to-building and building-for-grid services under uncertainty: A robust rolling horizon approach. IEEE Transactions on Smart Grid 13 (2), 1453–1467.

"Renewables.ninja." https://www.renewables.ninja/ (accessed.

Norlund, E.K., Gribkovskaia, I., 2017. Environmental performance of speed optimization strategies in offshore supply vessel planning under weather uncertainty. Transportation Research Part d: Transport and Environment 57, 10–22.

Peng, Y., Dong, M., Li, X., Liu, H., Wang, W., 2021. Cooperative optimization of shore power allocation and berth allocation: A balance between cost and environmental benefit. Journal of Cleaner Production. 10 (279), 123816.

Sarantakos, I., et al., 2022. A Robust Mixed-Integer Convex Model for Optimal Scheduling of Integrated Energy Storage—Soft Open Point Devices. IEEE Transactions on Smart Grid 13 (5), 4072–4087. https://doi.org/10.1109/TSG.2022.3145709.

Sarantakos, I., et al., 2023. Digitalization for Port Decarbonization: Decarbonization of key energy processes at the Port of Tyne. IEEE Electrification Magazine 11 (1), 61–72.

I. Sarantakos *et al.*, "Digitalization for Port Decarbonization (Accepted for Publication)," *IEEE Electrific. Mag.,* 2023.

Sha, M., et al., 2017. Scheduling optimization of yard cranes with minimal energy consumption at container terminals. Computers & Industrial Engineering 113, 704–713. https://doi.org/10.1016/j.cie.2016.03.022.

Starcrest Consulting Group, 2007. Port of Los Angeles inventory of air emissions 2005. Starcrest Consulting Group LLC, WA, USA.

Sun, X., Qiu, J., Tao, Y., Yi, Y., Zhao, J., 2022. Distributed Optimal Voltage Control and Berth Allocation of Electrified Ships in Seaport Microgrids. IEEE Trans. Smart Grid 13 (4), 2664–2674. https://doi.org/10.1109/TSG.2022.3161647.

Department for Transport. "Port freight statistics: notes and definitions." https://www.gov.uk/government/statistics/port-freight-annual-statistics-2021/port-freight-statistics-notes-and-definitions (accessed.

Wang, X., Huang, W., Wei, W., Tai, N., Li, R., Huang, Y., 2022. Day-Ahead Optimal Economic Dispatching of Integrated Port Energy Systems Considering Hydrogen. IEEE Trans. Ind. Appl. 58 (2), 2619–2629. https://doi.org/10.1109/TIA.2021.3095830.

Yu, J., VoB, S., Song, X., 2022. Multi-objective optimization of daily use of shore side electricity integrated with quayside operation. Journal of Cleaner Production 1 (351), 131406.

L. Yue, H. Fan, and C. Zhai, "Joint Configuration and Scheduling Optimization of a Dual-Trolley Quay Crane and Automatic Guided Vehicles with Consideration of Vessel Stability," *Sustainability*, vol. 12, no. 1, doi: 10.3390/su12010024.

Zeng, B., Zhao, L., 2013. Solving two-stage robust optimization problems using a column-and-constraint generation method. Oper. Res. Lett. 41 (5), 457–461. https://doi.org/10.1016/j.orl.2013.05.003.

Zhang, Y., Liang, C., Shi, J., Lim, G., Wu, Y., 2022. Optimal Port Microgrid Scheduling Incorporating Onshore Power Supply and Berth Allocation Under Uncertainty. Appl. Energy 313, 118856. https://doi.org/10.1016/j.apenergy.2022.118856.

Zhao, N., Schofield, N., Niu, W., 2016. Energy Storage System for a Port Crane Hybrid Power-Train. IEEE Trans. Transport. Electrific. 2 (4), 480–492. https://doi.org/10.1109/TTE.2016.2562360.